Hartree-Fock approximation for the *ab initio* no-core shell model

Mahmoud A. Hasan,[1] James P. Vary,[2] and Petr Navrátil[3]
[1]*Department of Physics, Applied Science University, Amman, Jordan*
[2]*Department of Physics and Astronomy, Iowa State University, Ames, Iowa 50011, USA*
[3]*Lawrence Livermore National Laboratory, Livermore, California 94550, USA*
(Received 13 September 2002; published 26 March 2004)

The spherical Hartree-Fock approximation is applied to the *ab initio* no-core shell model, with a realistic effective nucleon-nucleon interaction in order to investigate the range of its utility. Hartree-Fock results for binding energies, one-body density distributions, and occupation probabilities are compared with results from exact diagonalization in similar model spaces. We show that this mean-field approximation, especially with second-order corrections, is able to provide some useful approximations for ^{4}He and ^{16}O. We also explore the physical insights provided by the Hartree-Fock results for single-particle properties such as spin-orbit splittings. We find single-particle state ordering consistent with the phenomenological shell model.

DOI: 10.1103/PhysRevC.69.034332 PACS number(s): 21.60.−n, 21.45.+v, 27.10.+h, 27.20.+n

I. INTRODUCTION

Recently, the *ab initio* no-core shell model (NCSM) has been applied with realistic effective nucleon-nucleon (*NN*) interactions to light nuclei up to $A=12$ [1–4]. With the need to extend to heavier systems and to incorporate improvements such as effective and real three-body forces in ever larger model spaces, the prospect for near-term results is limited by present day computational resources. In light of this situation, there is a need for approximate methods to extend the *ab initio* NCSM to heavier systems with a wide range of observables to compare with experiment.

Hartree-Fock is a proven tool for semirealistic interactions for even the heaviest of nuclei [5] and is sufficiently flexible to handle many-body forces through the role of δ excitations [6–9]. It is also the starting point for practical many-body methods used extensively in heavier systems [5]. One of the new questions to address is the quantitative accuracy of Hartree-Fock itself when using the latest theories for effective interactions based on realistic *NN* potentials. Here, we provide an initial comparison in light nuclei which leads us to conclude that care must be exercised in the use of the mean-field approach with these newer effective Hamiltonians. The size of second-order corrections is found to be a useful gauge of the utility of the mean-field method in the present comparison.

Two recent efforts [10,11], taken together, show that the higher-order corrections to Hartree-Fock are rather sensitive to the choice of Hamiltonian. On the one hand, using phenomenological interactions, Ref. [10] presents higher-order corrections that are significantly smaller than those we obtain. These phenomenological interactions provide a good description of many experimental observables within the mean-field approach. It is not clear whether these phenomenological interactions would provide good descriptions of experiment in the NCSM approach or any other *ab initio* method. On the other hand, using a new method [12] to develop a realistic low-momentum nucleon-nucleon potential, called "$V_{low\text{-}k}$," Ref. [11] evaluated the Hartree-Fock results for ^{16}O and ^{40}Ca including corrections through third order. For ^{16}O the second-order corrections of Ref. [11] are somewhat larger than those we obtain. On the other hand, their Hartree-Fock results through third order are in better agreement with experiment. We discuss further the differences between our results and those of Ref. [11] in Sec. IV.

Of course, there is a long history going back to Brueckner, of merging the mean-field method with nonrelativistic effective potentials (G matrix) derived from *NN* interactions [13–15]. The conclusion of this extensive set of research is that such Hamiltonians underbind nuclei by about 1–3 MeV per nucleon. The tendency of the results is to have a root-mean-square radius r_{rms} which is too small compared to experiment whenever the binding energy approaches the experimental value ("Coester line").

Until recently, these extensive results left open the possibility that the mean-field method along with selected higher-order corrections, included by various means, was not a sufficiently accurate approach. However, with the advent of very precise methods to solve the many-fermion problem for light nuclei, there appears to be a good consensus now that the deficiency lies with the Hamiltonian itself. That is, we need true many-body forces to resolve the discrepancies between theoretical and experimental ground state (g.s.) properties.

Thus, we can easily imagine that properly constructed Hamiltonians, consisting of bare *NN* and *NNN* interactions, renormalized for large but finite basis spaces, could provide high precision descriptions of a wide variety of low-energy properties of nuclei. We then require many-body techniques that propel the applications in all nuclei, not just light nuclei. Given the recent advances in constructing such effective Hamiltonians, we may begin to reassess the utility of mean-field methods and their extensions for these purposes.

Our intent here is rather focused on a particular set of issues. We aim to examine the utility of the mean-field method with one of the more recent effective interaction approaches. We need to do this if we are to open the door to incorporating δ excitations as one of the important mechanisms for many-body forces in nuclei and if we are to proceed to heavier nuclei retaining predictive power. Indeed, we have been working in this direction for some time [6–9] with

effective Hamiltonians based on G matrices augmented by N-Δ and Δ-Δ interactions.

In the present effort, we have two specific goals: first, to compare spherical Hartree-Fock (SHF) with the *ab initio* NCSM in light nuclei where both methods are solvable with newly developed effective Hamiltonians in order to determine the quantitative accuracy of SHF and the associated conditions; second, to extract additional physical insights from SHF with these realistic effective Hamiltonians as a complement to the NCSM results.

II. THE EFFECTIVE HAMILTONIAN

The *ab initio* approach in shell-model studies of the nuclear many-body problem starts [1–4] with the intrinsic two-body Hamiltonian for the A-nucleon system, i.e.,

$$H = \sum_{i<j}^{A} [T_{ij} + V_{ij}], \tag{1}$$

with T_{ij} the relative kinetic energy between NN pairs and V_{ij} the NN interaction including the Coulomb interaction between protons. We ignore three-body interactions in the present effort. For the purposes of evaluating an effective Hamiltonian we modify it by adding (and later subtracting) the center-of-mass (c.m.) harmonic-oscillator (HO) Hamiltonian

$$H^{\Omega}_{\text{c.m.}} = \frac{\vec{P}^2}{2Am} + \frac{1}{2}Am\Omega^2\vec{R}^2, \tag{2}$$

with m the nucleon mass, $\vec{P}=\Sigma_{i=1}^{A}\vec{p}_i$, and $\vec{R}=(1/A)\Sigma_{i=1}^{A}\vec{r}_i$.

This addition/subtration of a single-particle potential, first introduced by Lipkin [16], helps our overall convergence when working in a HO set of basis states. We emphasize that it is important to ensure, as we do, that the *intrinsic* properties of the many-body system are not affected by the center-of-mass term. The modified Hamiltonian, thus, acquires a dependence on the HO frequency Ω, and can then be written as

$$H^{\Omega}_{A} = \sum_{i=1}^{A}\left[\frac{\vec{p}_i^{\,2}}{2m} + \frac{1}{2}m\Omega^2\vec{r}_i^{\,2}\right] + \sum_{i<j}^{A}\left[V_{ij} - \frac{m\Omega^2}{2A}(\vec{r}_i - \vec{r}_j)^2\right]. \tag{3}$$

Our shell-model calculations are performed in a model space defined by a projection operator P, with the complementary space (i.e., the excluded space) defined by the projection operator $Q=1-P$. Furthermore, due to its strong short-range part, the realistic nuclear interaction in Eqs. (1) and (3) will yield pathological results unless we derive a model-space dependent *effective* Hamiltonian

$$H^{\Omega}_{eff} = \sum_{i=1}^{A} P\left[\frac{\vec{p}_i^{\,2}}{2m} + \frac{1}{2}m\Omega^2\vec{r}_i^{\,2}\right]P + P[V_{eff}]P. \tag{4}$$

The effective interaction appearing in Eq. (4) is, in general, an A-body interaction, and, when it is obtained without any approximations, the model-space Hamiltonian provides an identical description of a subset of states as the exact original Hamiltonian [17,18].

From among the eigenstates of the Hamiltonian (4), it is necessary to choose only those that correspond to the same center-of-mass energy. This can be achieved by working in a complete $N_{max}\hbar\Omega$ model space, and then by shifting the center-of-mass eigenstates with energies greater than $\frac{3}{2}\hbar\Omega$ (representing spurious center-of-mass motion) upwards in the energy spectrum. We do this by adding $(\beta-1)PH^{\Omega}_{\text{c.m.}}P$ to and subtracting $\beta\frac{3}{2}\hbar\Omega P$ from Eq. (4) above. One unit of $H_{\text{c.m.}}$ has already been acquired, as mentioned above [4]. The resulting shell-model Hamiltonian takes the form

$$H^{\Omega}_{eff\,\beta} = \sum_{i<j}^{A} P\left[\frac{(\vec{p}_i - \vec{p}_j)^2}{2Am} + \frac{m\Omega^2}{2A}(\vec{r}_i - \vec{r}_j)^2\right]P + P[V_{eff}]P + \beta P\left(H^{\Omega}_{\text{c.m.}} - \frac{3}{2}\hbar\Omega\right)P, \tag{5}$$

where β is a sufficiently large positive parameter. When applied in a complete $N_{max}\hbar\Omega$ model space, this procedure removes the spurious center-of-mass motion exactly, and has no effect on the intrinsic spectrum of states with the lowest center-of-mass configuration [2].

In principle, the effective interaction introduced in Eqs. (4) and (5) above should reproduce exactly the full-space results in the model space for some subset of states. Furthermore, an A-body effective interaction is required for an A-nucleon system. In practice, however, the effective interaction cannot be calculated exactly, and it is approximated with a two-body effective interaction determined for a two-nucleon subsystem of the A-nucleon system. More recently, it has been possible to extend the effective interaction to the three-body cluster level [19].

In this work, we follow the procedure described in Refs. [2–4] in order to construct the two-body effective interaction. The procedure employs the Lee-Suzuki [17] similarity transformation method, which yields an interaction in the form

$$P_2V_{eff}P_2 = P_2VP_2 + P_2VQ_2\omega P_2, \tag{6}$$

with ω the transformation operator satisfying $\omega=Q_2\omega P_2$, and P_2 and $Q_2=1-P_2$ operators that project on the two-nucleon model and complementary spaces, respectively. Note that we distinguish between the two-nucleon system projection operators P_2, Q_2 and the A-nucleon system projection operators P, Q. The choice of P_2 is fixed by the choice of P. The remaining detailed steps to obtain the non-Hermitian form of H_{2eff} follow earlier work [3,4,17,18].

The final Hermitian form $\overline{H_{2eff}}$ is obtained by applying a similarity transformation determined from the metric operator $P_2(1+\omega^{\dagger}\omega)P_2$ [18]:

$$\overline{H_{2eff}} = [P_2(1+\omega^{\dagger}\omega)P_2]^{1/2}H_{2eff}[P_2(1+\omega^{\dagger}\omega)P_2]^{-1/2}. \tag{7}$$

The two-body effective interaction used in the present calculations is determined from this two-nucleon effective Hamiltonian as $V_{2eff}=\overline{H_{2eff}}-H^{\Omega}_{02}$, where H^{Ω}_{02} is the relative oscillator Hamiltonian for two particles. The resulting two-

body effective interaction V_{2eff} depends on A, on the HO frequency Ω, and on N_{max}, the maximum many-body HO excitation energy (above the lowest configuration) defining the P space. Furthermore, as discussed earlier, when used in the shell-model Hamiltonian (5), it results in the factorization of our many-body wave function into a product of a center-of-mass $0S$ component times an intrinsic component, which allows exact correction of any observable for spurious center-of-mass effects, thus preserving translational invariance. This feature distinguishes our approach from most phenomenological shell-model studies that involve multiple HO shells.

So far, the most important approximation used in our approach is the neglect of contributions coming from higher than two-body clusters to our effective Hamiltonian. In the NCSM the inclusion of a three-body effective interaction has been accomplished for $0s$- and $0p$- shell nuclei [19–21] though computational needs increase rapidly. For SHF it is straightforward, in principle, to carry out investigations with multibody effective Hamiltonians.

While the preservation of translational invariance in the NCSM is exact, this is not the case in our SHF approach. It is well known that projection before variation is desirable for obtaining optimized solutions respecting a given symmetry not already guaranteed by mean-field basis selection. Thus, it is possible to implement an exact treatment of translational invariance within Hartree-Fock [22]. Here, instead, we set $\beta=0$ in Eq. (5) and solve the conventional SHF problem. Since we introduce a SHF model-space truncation and we solve for a single slater determinant, our SHF results acquire c.m. motion dependence. Thus, our SHF rms radius and one-body density will have c.m. wave function smearing and we approximately correct for this in our rms radius results below.

The preservation of translational invariance in the effective Hamiltonian brings about a very interesting set of consequences for the mean-field single-particle energies [23]. Hence some care must be exercised in their interpretation and in comparison with results from other Hamiltonians.

For cases with either a purely intrinsic Hamiltonian (no one-body component) or a Hamiltonian with a one-body component plus intrinsic terms, we can list the common features. First, the single-particle energy is the eigenvalue of a mean-field one-body Hamiltonian equation derived from the application of the variational principle to the initial Hamiltonian. Second, it is this one-body self-consistent field problem that defines the leading order mean-field single-particle properties with which higher-order corrections are to be evaluated. Thus, in either case, it is the resulting single-particle energies that appear in the energy denominators of higher-order perturbation theory. Also, the associated single-particle wave functions are used to evaluate the matrix elements of the perturbative corrections. Third, in neither case may these single-particle energies be directly compared with experiment without considering the role of rearrangement. The single-particle energies and their associated rearrangement effects are not independent of each other and neither corresponds directly to an observable. Hence they may differ significantly between the two types of Hamiltonians.

We will now see why our single-particle energies differ substantially from those obtained with a combination of a one-body and a two-body Hamiltonian as conventionally employed. We will also see that we can easily extract results for spin-orbit splittings that are not markedly different from results of other approaches.

In particular, for our purely intrinsic effective Hamiltonians, we obtain a simple relationship between the Hartree-Fock (HF) energy and the single-particle energy:

$$E_{HF} = 0.5 \sum \epsilon_A (2j_A + 1), \tag{8}$$

where we signify orbits occupied in the slater determinant by capital roman letters. One can easily verify this relationship with the SHF results presented below. This relationship was already evident from thermal mean-field studies using pure two-body no-core Hamiltonians [24] and was examined in some detail in Ref. [23].

Herein lies an important bridge for comparing with experimental single-particle energies. In particular, by neglecting rearrangement effects, as is traditional when comparing mean-field results with experimental states in neighboring odd-mass nuclei, we see that the HF excitation energy is only one-half of the difference in the single-particle energies of a promoted particle. Thus if the difference in the single-particle energies between a particular single-particle state above the Fermi surface and one below, obtained with our intrinsic Hamiltonian, is 20 MeV, for example, then the Hartree-Fock energy of the associated Hartree-Fock excited state is just 10 MeV above the Hartree-Fock ground state.

To make the comparison with experiment more precise, we would need to carry out an evaluation of the rearrangement energy which takes us beyond the scope of the present effort. However, insofar as rearrangement effects may be neglected with both classes of Hamiltonians discussed above, it seems reasonable to compare one-half of our single-particle energy differences with full single-particle energy differences obtained from Hamiltonians having a one-body component. On this basis, we will compare quantitatively in Sec. IV the example of spin-orbit splittings obtained with our Hamiltonian and the results of Ref. [11] which employed a Hamiltonian with a one-body component.

As all Hartree-Fock energies are then proportional to the single-particle energies, we can obtain evidence on shell properties (single-particle state ordering and relative spacings) from the mean-field results with our chosen Hamiltonian. For example, the relative size of gaps between single-particle states can be used to determine where shell closures are predicted.

We select the CD-Bonn *NN* interaction [25,26] and include the Coulomb interaction between the protons. For ^{4}He we employ the 1996 CD-Bonn [25] while for ^{16}O we employ the 2000 CD-Bonn [26]. Where comparisons exist, the differences in these interactions are minor and are not expected to influence the results of our investigations.

Our selection of model-space sizes and harmonic-oscillator basis parameter are as follows: for both nuclei we conduct the SHF evaluations in a model space of six major shells. In addition, for ^{16}O we also provide results for model spaces of four and five major shells. For the NCSM, we

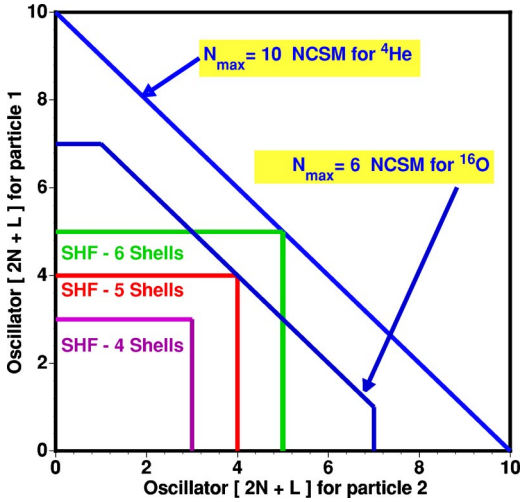

FIG. 1. (Color online) Depictions of the various P_2 space projectors defining the model spaces employed in the SHF and NCSM calculations.

select $N_{max}=10(^4\mathrm{He})$ and $N_{max}=6(^{16}\mathrm{O})$. For ^{4}He we use $\hbar\Omega=22$ MeV while for ^{16}O we use $\hbar\Omega=15$ MeV.

By way of explanation of the differences in model spaces sampled by SHF and by NCSM, we note that the model spaces are selected for a precise NCSM calculation with the evaluated H_{eff}. As a result, the SHF calculation samples a somewhat different basis space where all nucleons are allowed to be excited through a set of single-particle basis states depending on the number of oscillator shells included. Our philosophy is to fix H_{eff} and to use it for both the NCSM and SHF applications. In this way, we test how well the SHF results approximate the NCSM results, where the NCSM results are expected to converge to the exact answers as the model-space size increases. Figure 1 displays the two-particle model spaces employed in the SHF and NCSM for ^{4}He and ^{16}O. In areas where two-body effective Hamiltonian matrix elements are required for SHF but are absent in the NCSM, we simply use the relative kinetic energy matrix elements.

We solve for the properties of our selected nuclei using the SHF code underlying the results of Refs. [6–9] and the *m*-scheme Many-Fermion Dynamics code [27] which was developed for NCSM calculations.

In order to gauge the overall effectiveness of the SHF method, we also evaluate the second-order perturbative corrections to many observables presented here. We find the perturbative corrections significantly improve the agreement between SHF and NCSM as may be expected for closed shell systems. We label our perturbatively corrected results with "SHF(2)."

Let us specify the occupied SHF orbitals by capital roman letters and the unoccupied SHF orbitals by lower case roman letters. We allow for full charge dependence so that neutron and proton orbitals are separately indicated and we employ ϵ to signify the self-consistent SHF single-particle energies. Then, for example, we evaluate the second-order correction to the SHF binding energy

$$\Delta E_{SHF} = -\sum_{J,i\leq j,A\leq B}(2J+1)\frac{[\langle A_nB_n,J|H_{eff}|i_nj_n,J\rangle]^2}{\epsilon_{i_n}+\epsilon_{j_n}-\epsilon_{A_n}-\epsilon_{B_n}} - \sum_{J,i,j,A,B}(2J+1)\frac{[\langle A_nB_p,J|H_{eff}|i_nj_p,J\rangle]^2}{\epsilon_{i_n}+\epsilon_{j_p}-\epsilon_{A_n}-\epsilon_{B_p}} - \sum_{J,i\leq j,A\leq B}(2J+1)\frac{[\langle A_pB_p,J|H_{eff}|i_pj_p,J\rangle]^2}{\epsilon_{i_p}+\epsilon_{j_p}-\epsilon_{A_p}-\epsilon_{B_p}}, \quad (9)$$

where we signify reduced *jj*-coupled two-body matrix elements of the effective Hamiltonian in the SHF basis by $\langle ab,J|H_{eff}|cd,J\rangle$. In this shorthand notation, *a*, *b*, *c*, and *d* represent either occupied or unoccupied neutron or proton states. Our two-body states are normalized and antisymmetrized.

Furthermore, we evaluate the second-order correction to the occupation probabilities. We present the change in the occupation probability ΔN_{A_n} of the occupied SHF neutron orbital A_n as an example from which other cases $(\Delta N_{A_p},\Delta N_{i_n},\Delta N_{i_p})$ can easily be determined by appropriate modifications

$$\Delta N_{A_n} = \sum_{J,B,i\leq j}(2J+1)\frac{[\langle A_nB_n,J|H_{eff}|i_nj_n,J\rangle]^2}{(\epsilon_{i_n}+\epsilon_{j_n}-\epsilon_{A_n}-\epsilon_{B_n})^2} + \sum_{J,B,i,j}(2J+1)\frac{[\langle A_nB_p,J|H_{eff}|i_nj_p,J\rangle]^2}{(\epsilon_{i_n}+\epsilon_{j_p}-\epsilon_{A_n}-\epsilon_{B_p})^2}. \quad (10)$$

In every case, we verify by direct evaluation that the number of neutrons and the number of protons is separately conserved through the second-order calculations.

The second-order corrections to the SHF one-body density are easily evaluated from the corrections to the occupation probabilities. These corrections, in turn lead to a second-order correction to the rms radius.

We also introduce a standard correction to the SHF one-body density [14] to adjust the rms radius (RMS) for the spurious center-of-mass motion. This correction is defined as $\mathrm{RMS}=[(\mathrm{RMS}_{SHF})^2-b^2/A]^{1/2}$. For $A=4$ and 16 we use $b=1.374$ fm and 1.663 fm, respectively. All theoretical results for rms radii quoted here are for pointlike nucleons—i.e., we do not adjust for an electromagnetic radius of the nucleons. The sequence of corrections presented below begins with the second-order perturbative correction to the rms radius. We then apply the center-of-mass motion correction [quoted separately in the tables as Δ spur(c.m.)] to our SHF(2) result. The rms radius resulting from these corrections is also quoted in the tables below as the "Total."

In the following sections, we investigate several observables as well as properties of the wave functions. For observables, we evaluate the binding energy of the g.s. as well as its r_{rms}, one-body density distributions, single-particle energies, and occupation probabilities.

III. APPLICATION TO ^{4}He

In this section we apply the methods outlined in Sec. II to evaluate the properties of ^{4}He in the SHF and NCSM approaches.

TABLE I. Experimental and calculated observables for the ground state of ^{4}He with an $N_{max}=10$ effective Hamiltonian based on the 1996 CD-Bonn [25] and using $\hbar\Omega=22$ MeV. Experimental and calculated ground state energy (in MeV) and rms radii (in fm). The (negative) correction for spurious center-of-mass motion [Δ spur(c.m.)] is described in the text. For the experimental rms radius, we take the measured charge radius and correct for the contribution of the proton charge rms radius (0.8 fm).

Observable	Experiment	SHF Δ SHF Δ spur(c.m.)	SHF+ΔSHF +Δ spur(c.m.)	NCSM
$E_{\text{g.s.}}$	−28.296	−14.156 −10.835	−24.991	−27.913
n-rms		1.584		1.411
p-rms	1.450	1.590		1.416
rms		1.587 0.118 −0.145	1.560	1.413

For the NCSM, we use a complete $N_{max}\hbar\Omega$ model space with $N_{max}=10$ for the positive-parity states. This means that a total of 11 major harmonic-oscillator shells are involved. The two-nucleon model space shown in Fig. 1, is then defined by N_{max}, such that the restriction of the harmonic-oscillator single-particle states is given by $N_1=2n_1+l_1\leqslant N_{max}$, $N_2=2n_2+l_2\leqslant N_{max}$, and $(N_1+N_2)\leqslant N_{max}$. Thus, the maximum excitation of two nucleons simultaneously is through the sixth shell.

For the SHF we have a cutoff in basis states for each orbital—i.e., for each (lj) pair. Clearly, we would have to make some arbitrary choices if the SHF model space covers areas exceeding the NCSM space. We do make some attempts at this below where we examine the sensitivity to the choice of the SHF basis in more detail with the applications to ^{16}O. However, for ^{4}He we have selected the largest SHF basis included entirely within the $N_{max}=10$ space of the NCSM. Thus, we select the six-shell SHF basis shown in Fig. 1 that includes three *S* states, three *P* states, two *D* states, etc.

On the other hand, there is a range of two-body matrix elements of H_{eff} which participate in the NCSM calculations but not in the SHF calculations. To a certain degree, the present work tests the importance of those matrix elements for the g.s. properties of ^{4}He.

In Table I we present the experimental g.s. properties [28,29] along with the corresponding theoretical results from SHF and NCSM.

First, we note that the NCSM ground state energy is near the typical underbound result obtained with realistic interactions. In fact, the converged binding energy with the CD-Bonn *NN* potential is −26.30(15)MeV obtained in calculations that employ basis spaces up to $N_{max}=18$ [21]. At the same time, the SHF result appears to be rather far from NCSM with 13.76 MeV less binding. Most of this difference is recovered with the second-order corrections to SHF, that is the results of SHF(2), leaving a net 2.9 MeV difference. While the SHF(2) is considerably closer to the NCSM, the second-order correction may raise concern over the overall rate of convergence of the perturbative corrections to SHF for ^{4}He. We note, however, that the second-order correction is only 15.3% of the total SHF interaction energy [−70.946 MeV]. Hence, it appears reasonable to expect most of the remaining difference between SHF(2) and NCSM will be obtained in third order.

For the rms radii, the NCSM and SHF are rather close to each other and to experiment where it is available. The agreement between SHF(2) and NCSM is especially satisfying once the SHF(2) rms radius is corrected for spurious c.m. motion as described above.

In Table II we present occupation probabilities for selected orbitals. It is important to note that we present some results in the SHF basis and some in the HO basis. In particular, the first two columns present the probabilities that the neutron and proton orbitals are described by pure HO orbitals. The last two columns present the HO single-particle state occupation probability from the NCSM wave function. The intermediate two columns present the second-order correction to the ground state occupation probabilities *in the SHF basis*.

For ^{4}He, we observe rather good overlap of the SHF ground state with the lowest HO configuration. In addition, the NCSM indicates a rather pure HO lowest configuration description of the ground state. Hence there is overall close agreement. This agreement is retained since the SHF(2) corrections for the occupied $S_{1/2}$ orbital appear to be rather small. The unoccupied SHF orbitals indicate a strong degree of mixing but they do not directly contribute to the ground state SHF energy so this mixing is less relevant.

Overall, one feature is rather noticeable—the SHF wave function is less "correlated" than the NCSM ground state wave function. In the SHF basis, SHF(2) is encouraging with its trend indicating correlation mixtures approaching those of NCSM for the 0*S* orbital. At first glance, this comparison may appear a little dangerous as we are comparing results in a SHF basis with those in a HO basis. However, since the SHF occupied orbital is largely dominated by a single, HO orbit, the differences from the SHF occupation probabilities expressed in the HO basis would be negligible. This is the case, in general, for both light nuclei treated in the present work.

TABLE II. Selection of occupation probabilities for the ground state of ^{4}He. The columns "SHF" and "NCSM" label the probabilities in the HO basis. Specifically, in the case of the SHF unoccupied orbits, we quote their expansion probabilities in the HO basis. The Δ SHF columns present the second-order perturbative corrections in the SHF basis.

Orbital	SHF Neutron	SHF Proton	Δ SHF Neutron	Δ SHF Proton	NCSM Neutron	NCSM Proton
$0S_{1/2}$	0.992	0.991	−0.050	−0.050	0.941	0.940
$1S_{1/2}$	0.005	0.005	0.002	0.002	0.008	0.008
$2S_{1/2}$	0.004	0.005	0.000	0.000	0.003	0.003
$0P_{3/2}$	0.794	0.784	0.007	0.007	0.004	0.004
$0P_{1/2}$	0.629	0.621	0.014	0.015	0.016	0.016
$0D_{5/2}$	0.833	0.829	0.000	0.000	0.001	0.001
$0D_{3/2}$	0.764	0.761	0.002	0.002	0.002	0.002

In Table III we present the SHF single-particle energies for ^{4}He. We note again that the single-particle energies cannot be compared directly with the experimental separation energies without considering the expected large rearrangement effects.

Our spectrum of single-particle energies is shifted about 20 MeV from the results obtained with phenomenological Hamiltonians that include a one-body part. This shift has been addressed [23] in some detail and is related to the role of the c.m. motion. Our single-particle energies contain a contribution of $\approx\langle T_{rel}/A\rangle$ where the expectation value is with respect to the self-consistent single-particle wave function.

Recalling the factor of one-half discussed in the preceding section, we may interpret the results of Table III as predicting a $0P_{3/2}-0S_{1/2}$ particle-hole excited state of ^{4}He, neglecting rearrangement effects, at about $34.6/2=17.3$ MeV. This is low compared to the lowest negative-parity excited state involving this configuration at 21.84 MeV of excitation.

We present the radial one-body density distributions for ^{4}He in Fig. 2. One is struck by the apparent large differences between the mean-field, either SHF or SHF(2), and the NCSM distributions. Overall, the distributions presented are similar in shape but appear scaled by an amount indicated by their rms radii (see Table I). We shall see below that such a simple scaling does not appear in ^{16}O.

One major difference between our mean-field radial distributions compared with NCSM is due to a spurious center-of-mass smearing effect present in our mean-field results. We anticipate that as we proceed to heavier systems, one of our major goals, this spurious effect will be less significant.

TABLE III. SHF single-particle energies for the ground state of ^{4}He in a six-shell-model space using $\hbar\Omega=22$ MeV.

Orbital	Neutron	Proton
$0S_{1/2}$	−7.546	−6.610
$0P_{3/2}$	27.156	28.218
$0P_{1/2}$	30.409	31.367
$0D_{5/2}$	40.877	41.855
$1S_{1/2}$	35.955	36.936
$0D_{3/2}$	43.003	43.947

Some differences between SHF and NCSM results are due to the different model spaces using the $10\hbar\Omega$ NCSM effective Hamiltonian derived for ^{4}He as depicted in Fig. 1. Below, we will investigate the significance of different model spaces using the ^{16}O case with a $6\hbar\Omega$ effective Hamiltonian derived for the NCSM space.

IV. APPLICATION TO ^{16}O

For ^{16}O, we conduct the NCSM investigations in a $6\hbar\Omega$ model space, the largest that is currently feasible for this nucleus. In the *m* scheme, for $M=0$ configurations, the $6\hbar\Omega(8\hbar\Omega)$ basis dimensionality is 26,483,625 (996,878,170) for this nucleus. We conduct the SHF calculations in a series of three model spaces (four shells, five shells, and six shells) that cover a range of situations both smaller and larger in certain aspects than the NCSM space. These selections are compared in Fig. 1.

In the six-shell space, the SHF is missing certain matrix elements due to the limitations of the NCSM space. This corresponds to the region where the SHF model space contains two-nucleon excitations beyond the NCSM space.

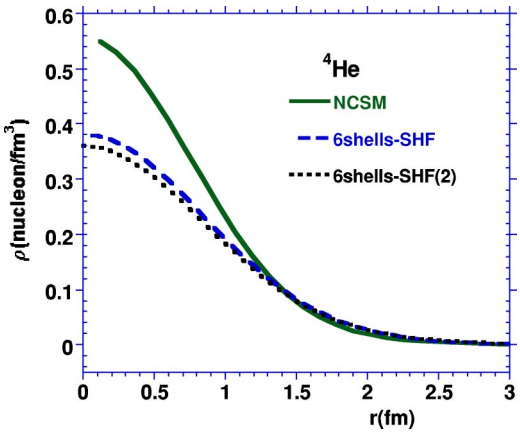

FIG. 2. (Color online) One-body radial density distributions obtained in the SHF and NCSM calculations for ^{4}He.

TABLE IV. Experimental and calculated observables for the ground state of ^{16}O with an $N_{max}=6$ effective Hamiltonian based on the 2000 CD-Bonn [26] and using $\hbar\Omega=15$ MeV. Experimental and calculated ground state energy (in MeV) and rms radii (in fm). The (negative) correction for spurious center-of-mass motion [Δ spur(c.m.)] is described in the text. For the experimental rms radius, we take the measured charge radius and correct for the contribution of the proton charge rms radius (0.8 fm). SHF results are presented for four-shell-, five-shell-, and six-shell-model spaces.

Observable [Experiment]	four-shell SHF Δ SHF Δ spur(c.m.) Total	five-shell SHF Δ SHF Δ spur(c.m.) Total	six-shell SHF Δ SHF Δ spur(c.m.) Total	NCSM
$E_{\text{g.s.}}$	−107.46	−109.83	−126.00	−132.87
[−127.62]	−31.46	−49.88	−38.21	
	−138.92	−159.71	−164.21	
n-rms	2.093	2.071	1.954	2.209
p-rms	2.101	2.080	1.968	2.223
[2.58]				
rms	2.097	2.076	1.961	2.216
	0.072	0.112	0.117	
	−0.040	−0.040	−0.042	
	2.129	2.148	2.036	

When this occurs in our SHF calculations, the V_{eff} matrix elements vanish while we do retain the unrenormalized relative kinetic energy matrix elements.

In Table IV we present the experimental and theoretical ground state properties for ^{16}O. We examine the dependence of the SHF results on the number of shells included in such a way as to bracket the division in model space accomplished in the corresponding NCSM results as shown in Fig. 1.

The SHF ground state energy is between 7 and 25 MeV above the NCSM result. When we include the SHF(2) corrections, the differences are altered to a range of 6–32 MeV. The larger these corrections, the more significant they are as indicators of possible difficulties with a convergent perturbation theory based on SHF for this nucleus. However, when viewed on the scale of the total interaction energy, these concerns are reduced. The second-order correction is $[6.5\%, 10.1\%, 6.9\%]$ of the total SHF interaction energy $[-481.01, -492.37, -554.61]$ MeV in the [4–6] shell-model spaces, respectively. In all these ^{16}O cases, the small percentage change when including second-order corrections is encouraging for our goal of treating heavier systems in SHF(2).

We note from the binding energies in Table IV that the SHF results are closest to NCSM in the six-shell case while, with second-order corrections, the four-shell results are closest.

Let us also address the issue of convergence by comparing the size of our second-order corrections in ^{16}O with the perturbative corrections obtained in Ref. [11] using a different approach and featuring a realistic smoothed nucleon-nucleon interaction, $V_{low\text{-}k}$ [12]. They obtain a second-order correction that is 17% of their total SHF interaction energy of −376 MeV and a third-order correction of 8%. We note that the average of our second-order corrections (7.8%) is comparable in percentage to their third-order correction.

Table V presents for ^{16}O the occupation probabilities for selected orbitals in the six-shell SHF calculations and compares them with the $N_{max}=6$ results of the NCSM. We see that SHF shows greater mixing in the SHF occupied orbits than does NCSM which provides a distinctive situation from that observed above for ^{4}He.

The second-order corrections to the SHF occupation probabilities presented in Table V are all small and consistent with a well-behaved perturbation theory. As a figure of merit, we note that the total neutron and proton percentage promoted from occupied to unoccupied orbits is about 5% in the four-shell case while increasing slightly in the five-shell and six-shell SHF results. Hence, the concern raised above with the apparent large second-order corrections to the SHF energy is again reduced.

We present the ^{16}O single-particle energies in Table VI for the four-, five-, and six-shell SHF results. We again cite our warning about direct comparison between these single-particle energies and experimental states in odd-mass neighboring nuclei.

First, we note that the Hartree-Fock energy difference for the neutron orbits, $0D_{5/2}-0P_{1/2}$, is $(23.6, 22.4, 24.7)/2 = (11.8, 11.2, 12.4)$ MeV in the four-, five-, and six-shell results, respectively. These values compare favorably with the experimental neutron $0D_{5/2}$-$0P_{1/2}$ splitting of 11.52 MeV obtained from the binding energy differences of ^{17}O and ^{15}O. Similar results are obtained when comparing the proton SHF single-particle energies with experimental binding energies of neighboring odd nuclei after accounting for Coulomb corrections. The proton $0D_{5/2}$-$0P_{1/2}$ splittings are $(23.3, 22.4, 24.5)/2 = (11.7, 11.2, 12.3)$MeV in the four-, five-, and six-shell results, respectively. The relevant experimental splitting is 11.53 MeV. Thus, the size of the gap be-

TABLE V. Selection of occupation probabilities for the ground state of ^{16}O with an $N_{max}=6$ effective Hamiltonian using $\hbar\Omega=15$ MeV. The SHF calculations were performed in the six-shell space. The column SHF and NCSM labels the probabilities in the HO basis. Specifically, in the case of the SHF unoccupied orbits, we quote their expansion probabilities in the HO basis. The Δ SHF labels the second-order perturbative corrections in the SHF basis.

Orbital	SHF Neutron	SHF Proton	Δ SHF Neutron	Δ SHF Proton	NCSM Neutron	NCSM Proton
$0S_{1/2}$	0.887	0.892	−0.020	−0.019	0.959	0.961
$1S_{1/2}$	0.102	0.098	0.015	0.014	0.033	0.031
$2S_{1/2}$	0.012	0.011	0.000	0.000	0.003	0.003
$0P_{3/2}$	0.843	0.851	−0.041	0.040	0.935	0.939
$1P_{3/2}$	0.131	0.125	0.006	0.005	0.032	0.029
$2P_{3/2}$	0.025	0.024	0.002	0.002	0.004	0.004
$0P_{1/2}$	0.886	0.895	−0.079	−0.079	0.938	0.941
$1P_{1/2}$	0.087	0.079	0.004	0.004	0.020	0.018
$2P_{1/2}$	0.027	0.026	0.000	0.000	0.004	0.004
$0D_{5/2}$	0.955	0.965	0.013	0.013	0.013	0.013
$0D_{3/2}$	0.978	0.964	0.017	0.019	0.015	0.015

tween the occupied and unoccupied SHF states that we find in ^{16}O is in accord with the known doubly magic character of this nucleus. We also note that Ref. [11] obtains the corresponding (full) single-particle energy splitting of 15.6 MeV.

In a similar vein, and with similar caution, we may examine our spin-orbit splittings. For example, the four-, five-, and six-shell neutron $0P_{3/2}$-$0P_{1/2}$ splittings of Table VI are $(10.0, 10.9, 13.9)/2=(5, 5.5, 7)$MeV, respectively, which are in approximate agreement with the experimental splitting in ^{15}O of 6.2 MeV. We note that Ref. [11] obtains a spin-orbit splitting of 7.6 MeV for these P states.

A corresponding comparison of the neutron $0D_{5/2}$-$0D_{3/2}$ splittings yields $(9.6, 10.4, 11.5)/2=(4.8, 5.2, 5.8)$MeV in comparison with the experimental splitting of 5.1 MeV and the result of 5.9 MeV in Ref. [11].

In Fig. 3 we present the radial one-body density distributions for ^{16}O obtained in the NCSM and SHF calculations. Here we note significant differences between SHF and NCSM, especially in the central region. It is worth commenting that our SHF results are quite consistent with long-established results of Brueckner Hartree-Fock [14] and coupled cluster [30]. In fact our NCSM results are somewhat closer to the traditional results from density dependent Hartree-Fock either with phenomenological interactions [31] or with higher-order Brueckner approaches such as renormalized Brueckner Hartree-Fock [15]. Hence, the more surprising result is the NCSM smooth Gaussian-like shape (solid line). This implies that simple scaling cannot reduce the differences between SHF and NCSM in the case of ^{16}O.

V. CONCLUSIONS AND OUTLOOK

We have compared results obtained with exact diagonalization in large multishell-model spaces (*ab initio* no-core shell model) with the approximate results from spherical Hartree-Fock using realistic effective two-body Hamiltonians. Significant differences are obtained and second-order corrections to SHF bring the SHF into reasonable agreement with NCSM for ^{4}He and ^{16}O in SHF model spaces "enclosed" by the NCSM space. By enclosed we refer to the sketch of model spaces in Fig. 1 where the meaning is clear from the labeled model spaces.

One recent effort [10], with which we can compare our results, shows that higher-order corrections to Hartree-Fock using phenomenological interactions are significantly smaller than those we obtain here. It is reasonable, in our view, that

TABLE VI. SHF single-particle energies for the ground state of ^{16}O in a four-shell-, five-shell-, and six-shell-model spaces using $\hbar\Omega=15$ MeV.

Orbital	four-shell Neutron	four-shell Proton	five-shell Neutron	five-shell Proton	six-shell Neutron	six-shell Proton
$0S_{1/2}$	−41.877	−37.402	−44.289	−39.714	−49.101	−44.312
$0P_{3/2}$	−10.148	−5.893	−10.085	−5.778	−12.334	−7.743
$0P_{1/2}$	−0.129	4.031	0.852	5.042	1.575	5.997
$0D_{5/2}$	23.437	27.335	23.277	27.450	26.261	30.537
$1S_{1/2}$	24.840	28.614	25.037	28.842	28.255	32.075
$0D_{3/2}$	33.080	36.920	33.650	37.295	37.803	40.991

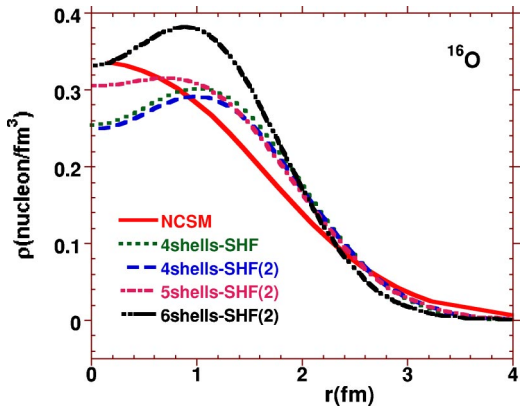

FIG. 3. (Color online) One-body radial density distributions obtained in the SHF and NCSM calculations for ^{16}O.

the rates of convergence of higher-order corrections to SHF are different between realistic effective Hamiltonian approaches and phenomenological interactions.

These phenomenological interactions have been adjusted within Hartree-Fock to provide a good description of many experimental observables using the mean-field approximation. For the NCSM, we now understand that residual differences between theory and experiment in light nuclei are due to contributions from effective and real three-body forces. How possible differences between NCSM theory and experiment will be resolved in heavier systems will require further investigation.

Another recent effort [11], with which we can also compare our results, shows somewhat larger higher-order corrections to Hartree-Fock using a different realistic effective Hamiltonian. The resulting mean-field excitation spectra of ^{16}O are rather similar considering the differences in our approaches. With the caveat that rearrangement corrections are not included, both approaches give spin-orbit splittings in rough accord with experiment. Our mean-field rms radii are somewhat smaller than those of Ref. [11] and smaller than experiment but our mean-field rms radii approximately agree with the NCSM results. This raises additional questions regarding the different mean-field treatments of the c.m. motion.

Additional questions worth examining in the future include making a similar comparison between SHF and NCSM with effective three-body Hamiltonians including true three-body forces. It is anticipated that such additional study will be especially worthwhile if the expected improved agreement between theory and experiment with realistic effective Hamiltonians is achieved.

We also conclude that investigations of heavier closed shell nuclei with SHF(2) are now warranted where the NCSM results are not obtainable in the near future.

ACKNOWLEDGMENTS

M.A.H. and J.P.V. acknowledge partial support from NSF Contract No. INT00-80491. J.P.V acknowledges support from U.S. DOE Grant No. DE-FG02-87ER-40371. This work was performed in part under the auspices of the U.S. Department of Energy by the University of California, Lawrence Livermore National Laboratory under Contract No. W-7405-Eng-48. P.N. acknowledges support from LDRD Contract No. 00-ERD-028.

[1] D. C. Zheng, B. R. Barrett, J. P. Vary, W. C. Haxton, and C.-L. Song, Phys. Rev. C **52**, 2488 (1995).
[2] P. Navrátil and B. R. Barrett, Phys. Rev. C **54**, 2986 (1996).
[3] P. Navrátil, J. P. Vary, and B. R. Barrett, Phys. Rev. Lett. **84**, 5728 (2000).
[4] P. Navrátil, J. P. Vary, and B. R. Barrett, Phys. Rev. C **62**, 054311 (2000).
[5] P. Ring and P. Schuck, *The Nuclear Many Body Problem* (Springer, Berlin, 1980), and references therein.
[6] M. A. Hasan, T.-S. H. Lee, and J. P. Vary, Phys. Rev. C **56**, 3063 (1997).
[7] M. A. Hasan, S. Kohler, and J. P. Vary, Phys. Rev. C **36**, R2180 (1987); **36**, 2649 (1987); J. P. Vary and M. A. Hasan, Phys. Rep. **242**, 139 (1994); Nucl. Phys. **A570**, 355 (1994); M. A. Hasan and J. P. Vary, Phys. Rev. C **50**, 202 (1994); **54**, 3035 (1996).
[8] M. A. Hasan, Dirasat (University of Jordan, Jordan, 1995), Vol. 22B, No. 3, pp. 777–804.
[9] M. A. Hasan, J. P. Vary, and T.-S. H. Lee, Phys. Rev. C **61**, 014301 (1999); **64**, 024306 (2001).
[10] P. Stevenson, M. R. Strayer, and J. R. Stone, Phys. Rev. C **63**, 054309 (2001).
[11] L. Coraggio, N. Itaco, A. Covello, A. Gargano, and T. T. S. Kuo, Phys. Rev. C **68**, 034320 (2003).
[12] S. Bogner, T. T. S. Kuo, and L. Coraggio, Nucl. Phys. **A684**, 432c (2001); S. Bogner, T. T. S. Kuo, L. Coraggio, A. Covello, and N. Itaco, Phys. Rev. C **65**, 051301(R) (2002).
[13] B. D. Day, Rev. Mod. Phys. **39**, 719 (1967).
[14] J. W. Negele, Phys. Rev. C **1**, 1260 (1970).
[15] K. T. R. Davies and R. J. McCarthy, Phys. Rev. C **4**, 81 (1971), and references therein.
[16] H. J. Lipkin, Phys. Rev. **109**, 2071 (1958).
[17] K. Suzuki and S. Y. Lee, Prog. Theor. Phys. **64**, 2091 (1980).
[18] K. Suzuki, Prog. Theor. Phys. **68**, 246 (1982); K. Suzuki and R. Okamoto, *ibid.* **70**, 439 (1983).
[19] P. Navrátil and W. E. Ormand, Phys. Rev. Lett. **88**, 152502 (2002).
[20] P. Navrátil and B. R. Barrett, Phys. Rev. C **57**, 562 (1998); **57**, 3119 (1998).
[21] P. Navrátil, G. P. Kamuntavicius, and B. R. Barrett, Phys. Rev. C **61**, 044001 (2000).
[22] K. W. Schmid, Eur. Phys. J. A **14**, 413 (2002), and references therein.
[23] L. Jaqua, M. A. Hasan, J. P. Vary, and B. R. Barrett, Phys. Rev. C **46**, 2333 (1992).
[24] G. Bozzolo, O. Civitarese, and J. P. Vary, Phys. Rev. C **37**,

1240 (1988).
[25] R. Machleidt, F. Sammarruca, and Y. Song, Phys. Rev. C **53**, 1483 (1996).
[26] R. Machleidt, Phys. Rev. C **63**, 024001 (2001).
[27] J. P. Vary, The-many-Fermion-Dynamics Shell-Model Code, Iowa State University, 1992 (unpublished); J. P. Vary and D. C. Zheng, The-Many-Fermion-Dynamics Shell-Model Code, Iowa State University, 1994 (unpublished).
[28] G. Audi and A. H. Wapstra, Nucl. Phys. **A595**, 409 (1995).
[29] National Nuclear Data Center, http://www.nndc.bnl.gov
[30] H. Kuemmel, K. H. Luehrmann, and J. G. Zabolitsky, Phys. Rev. C **36**, 1 (1978).
[31] D. Vautherin and D. M. Brink, Phys. Rev. C **5**, 626 (1972).